

KINETICS AND MECHANISM
OF CHEMICAL REACTIONS. CATALYSIS

Studying the Mechanism of the Low-Temperature Oxidation of Microsized Aluminum Powder by Water

N. S. Shaitura^{a,*}, O. O. Laricheva^a, and M. N. Larichev^a

^aTalozhe Institute of Energy Problems of Chemical Physics, Russian Academy of Sciences,
Leninskii pr. 38/2, Moscow, 119334 Russia

*e-mail: tesh-s@yandex.ru

Received July 26, 2018; revised September 5, 2018; accepted September 20, 2018

Abstract—The mechanism of the oxidation of disperse aluminum (powder of ASD-4 grade) by liquid water was studied including the use of different process activation methods (thermal, ultrasonic, and chemical in the presence of small CaO amounts). For this purpose, the complex study of the aluminum oxidation process was performed at its different stages by analyzing the kinetic dependences of the hydrogen formation rate and the reaction medium pH change and using the instrumental methods of scanning electron microscopy and X-ray diffraction analysis. It has been demonstrated that the shape of kinetic hydrogen release curves, the oxidation process completeness, and the structure of formed hydroxides are interrelated. An essential role is played by the mass transfer of formed solid oxidation products from the surface of particles to the crystallization nuclei of aluminum hydroxide and the localization of crystallization areas. This work is topical because of the broad interest in the use of metallic aluminum as an energy-accumulating substance.

Keywords: disperse aluminum, oxidation by water, aluminum hydroxide, hydrogen synthesis, hydrogen energetics, hydrogen generator

DOI: 10.1134/S1990793119020088

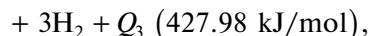
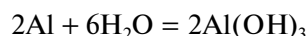
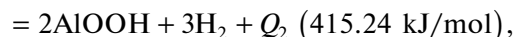
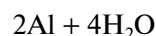
1. INTRODUCTION

Metallic aluminum is a highly reactive metal, whose oxidation occurs with the release of considerable specific heat comparable with the calorific value of the best grades of coal. Owing to this fact, the possibility of using metallic aluminum as a highly efficient energy-accumulating material, in which the accumulation of energy occurs via the reduction of this metal from its oxide (the most widespread form of the element aluminum in the Earth's crust), and the release of energy that occurs via the oxidation of aluminum, has been widely studied in the last decade [1–5]. Because the reduction of metallic aluminum from its oxide is an energy-consuming process, it is implied that the production of aluminum will be organized in the areas of a higher concentration of renewable energy sources. Aluminum can be easily and safely transported to the places of its utilization and stored for a long time. The application of aluminum as an energy carrying material is an environmentally friendly process intended for use in the most energetically loaded regions (megapolises) and areas without centralized energy supply.

Due to its high chemical activity, aluminum can react with different oxidants (O₂, N₂, CO₂, H₂O) with the release of heat and the formation of corresponding solid products at corresponding heat effects and form

some other chemical compounds, which in turn may be used as energy-carrying materials. The latter are exemplified by hydrogen, which is formed in the reaction of aluminum with water and can be used for the needs of hydrogen energetics. The use of aluminum for the production of hydrogen is promising especially in mobile power generation systems.

The products of the reaction between aluminum and water are hydrogen, heat, and solid oxidation products. The heat effects and the composition of solid oxidation products depend on the process conditions, and the amount of released hydrogen is the same for all the reaction channels



and attains nearly 11% from the mass of reacting aluminum or 3.7% from the total mass of metal and water. This percentage is rather high for aluminum to be seriously considered as a promising hydrogen-accumulating compound. Solid oxidation products (aluminum oxides and hydroxides) can be used as recyclable

materials for the recovery of metallic aluminum. However, the economic efficiency of the production of gaseous hydrogen from aluminum may be increased in the case if the solid oxidation products can be used in improved consumer properties, which supply their use in other branches of industry. This subject is highlighted, in particular, in the works [6, 7] studying the conversion of aluminum oxyhydroxide synthesized via the hydrothermal oxidation of aluminum into valuable highly pure aluminum oxide and its properties. The ultrasonic activation of the aluminum oxidation process with the possibility to perform the complete oxidation of microsized aluminum powders by water without chemical activators contaminating the oxidation products alongside with the synthesis of aluminum hydroxide of different structure (including nano-sized one) was proposed by the authors of this work in [8–12].

Since the aluminum oxidation reaction is heterogeneous, the size and shape of aluminum powder particles [13] and the composition and state of a passivating oxide coating (POC) on their surface [13–15] have an essential impact on the oxidation process kinetics. Such a coating results from the oxidation of the surface metal layer by atmospheric oxygen and atmospheric moisture molecules, attains the thickness providing its impermeability for gases, and protects the metal from further oxidation. Its thickness usually reaches several nanometers [16].

The low-temperature oxidation of aluminum seems to be the simplest and most safe implementation of the process. It is known that the low-temperature oxidation of aluminum by distilled water without activation is characterized by a very long induction period (up to several days at room temperature) and a low degree of metal oxidation. For this reason, the objectives of activation methods are:

—to destruct the passivating oxide coating existing on the surface of metallic aluminum; and

—to overcome the passivating effect created by solid oxidation reaction products, which are continuously formed on the oxidized metal surface.

A number of activation methods detailed in the papers [2–5] have been proposed for the activation of the aluminum oxidation process to date. When selecting the promising activation methods, we took into account their environmental friendliness, i.e., the possibility to perform the aluminum oxidation process without contaminating the formed oxidation products and the environment. As mentioned above, this requirement is completely satisfied by ultrasonic activation and, as shown in the work [9], by the use of CaO as a chemical activator. In the latter case, the contamination of formed aluminum hydroxide will be determined by the amount of the used activating reagent. For this reason, the described studies were focused on the possibility to use CaO activator additives in the

amounts, which were usually less than 5% of the mass of oxidized Al.

The mechanism of aluminum oxidation was studied by a number of authors in the works [15, 17–20]. Despite the earlier results, many aspects and regularities of oxidation remain unclear. In particular, when studying the activation of this process by small CaO additives or/and ultrasound, the authors of this work obtained the kinetic hydrogen formation curves with one, two and, in some cases, three maxima. Moreover, as established in [9], an increase in the oxidation process temperature leads to a nonlinear change in such parameters as the average aluminum oxidation rate and degree. The literature data available for the authors do not provide any explanation of these features, so the objective of this work was to study the process mechanism and, in particular, to explain the regularities established earlier.

2. MATERIALS AND METHODS

The oxidation of ASD-4 aluminum powder (*TU* (Technical Specification) 48-5-226-87), which is commercially produced by the Russian industry, with an average size of spherical particles of nearly 4 μm [9] was studied in this work. The surface of particles had a POC. The selection of this powder for study was stipulated by its practical application prospects in the production of hydrogen, i.e., its relatively low cost, availability, and convenient storage and transportation. According to *TU 48-5-226-87*, the content of active aluminum in powder particles is 99.1%, as confirmed by the data of performed volumetric analysis.

According to the nominal data, the major admixtures are Fe (100 ppm), Si (80 ppm), and Mg (8 ppm). The real admixture composition determined by spark mass spectrometry on a JEOL JMS-01 BM-2 spectrometer may slightly differ from the nominal composition [21]. The absence of appreciable distinctions between the results of kinetic measurements on the oxidation of powders from different batches by liquid distilled water allows us to state that the difference in the composition of admixtures is not essential for the studied oxidation process.

In this work, distilled water was used as an oxidizer. The ratio of the reagents Al : H₂O in the experiments varied from 1 : 2 to 1 : 25 (wt %). The oxidation process was chemically activated using CaO of chemically pure grade (content, no less than 99 wt %).

The aluminum oxidation was studied at nearly atmospheric pressures and temperatures below 100°C. The oxidation of aluminum powder of ASD-4 grade by water was studied on the setups detailed in the work [9]. The oxidation was studied both in the nearly isothermal regime, when the temperature of the external walls of the chemical reactor was maintained at a specified level (quasi-isothermic regime) and the heat accumulation regime, in which the external reactor

walls were thermally insulated (see [9] for more details on the implementation of these regimes).

The initial aluminum powder and the solid products of its oxidation by water were studied by scanning electron microscopy (SEM) on a JSM-7401F microscope. The X-ray diffraction analysis of samples was performed on a Bruker D8 ADVANCE diffractometer. X-ray diffraction patterns were refined using the TOPAS-4.2 full-profile analysis software. The size of microcrystallites was determined from the coherent scattering regions. The crystallinity of a sample was calculated from the comparison of integral intensities for the peaks of crystalline and amorphous components.

A sample for SEM and X-ray diffraction analysis was taken at different reaction stages in the form of a small reaction mixture amount (several milligrams), which was quickly dried in a dry air flow (for 20–30 s). This provided the possibility to stop the oxidation process just at the stage, which was attained by this process in the reactor.

Medium pH was measured on a Metrohm 692Ion/pH meter using a Pt electrode providing pH measurements within a range of 0–14 at a temperature of 0–80°C.

3. RESULTS AND DISCUSSION

The process of aluminum oxidation by water can be conditionally divided into several consecutive stages overlapping each other and, under certain oxidation conditions, represent alternating stages, among which we should distinguish the following ones [1, 4] (Fig. 1):

—The initial oxidation stage representing a rapidly damping reaction, which occurs with the release of a small H_2 amount, is detected for the first minutes of contact between aluminum powder and water, and results in the oxidation of metal up to several percent and a short-term increase in the temperature (up to several degrees) in the mixture of reagents.

—The induction stage (with the duration from several minutes to several days depending on the composition and structure of the POC of powder particles, the starting reaction temperature, and pH of the reaction medium), during which the POC is subjected to hydrolysis, which destroys the integrity of POC and increases its permeability for water molecules. The end of the induction period is characterized by the beginning of growth in the hydrogen release rate and an increase in the reaction mixture temperature, which indicates the beginning of the intensive metal oxidation stage.

—The intensive oxidation stage, during which the hydrogen release rate quickly increases due to the intensive destruction of the POC and an increase in the reaction mixture temperature. In addition to hydrogen, the formation and accumulation of solid aluminum oxidation products takes place.

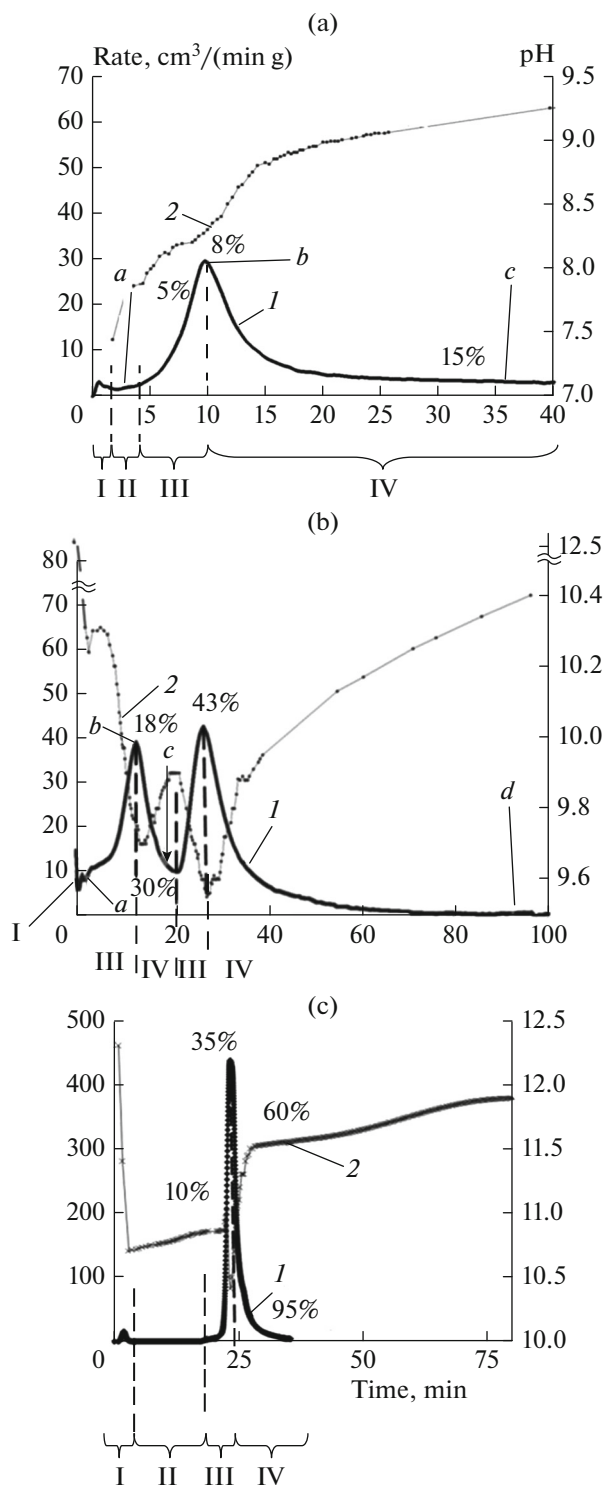


Fig. 1. Characteristic kinetic curves of (1) the hydrogen release rate and (2) pH of the medium for (a) the isothermic oxidation regime at starting pH 7, (b) the isothermic oxidation regime at starting pH 12.5, and (c) the heat accumulation regime at starting pH 12.5 (the letters are the points of sampling for electron microscopy (Figs. 2, 5)). Aluminum conversion during the process is given in %. Oxidation process stages: (I) initial oxidation stage, (II) induction stage, (III) intensive oxidation stage, (IV) oxidation damping stage.

—The oxidation process damping stage determined by that the geometric non-oxidized aluminum surface contacting with the oxidizer is reduced in the system during the oxidation process. Moreover, the formed insoluble oxidation products hamper the transport of water to the reaction zone. Due to this set of facts, the rate of metal oxidation begins to decrease from a certain moment, simultaneously provoking a decrease in the reaction mixture temperature and the liberated hydrogen amount.

Experimental data show that the kinetic gas release rate curve can have one (Figs. 1a and 1c), two (Fig. 1b), and even three gas release maxima depending on the oxidation process conditions. In the case of several such maxima, the process damping stage evolves into the intensive oxidation stage again. Let us consider the processes occurring at each stage in more details.

Initial Oxidation and Induction Stages

As shown in the work [4], the initial oxidation stage is observed for the several first minutes of contact between aluminum powder and water and explained by the existence of a certain amount of POC structure defects, which are impermeable for atmospheric oxygen, but open upon contact with liquid water, e.g., due to the Reh binder effect [22]. The essence of this effect consists in that the physicochemical interaction of an adsorptionally active medium with the surface of solids leads to an appreciable change in the mechanical properties of crystals and amorphous materials of different nature, i.e., the POC is destructed in defective areas upon contact with water. Another possible reason for the destruction of the POC is its dissolution, which will locally occur in the most defective POC areas. At medium pH > 7, the dissolution of aluminum oxide generally occurs with the formation of $[\text{Al}(\text{OH})_4]^-$ ions [23] and incorporates two stages, (1) the hydration of oxide and (2) the dissolution of formed aluminum hydroxide.

Let us consider the possible nature of POC structure defects. According to X-ray diffraction data, an aluminum particle has a microcrystalline structure with a grain size of nearly 0.1–0.2 μm . This means that it represents differently oriented microcrystallites bonded together by amorphous metal areas. For this reason, the surface of a particle has a patchwork structure composed of differently oriented outcropping crystal faces and thin amorphous aluminum areas binding them. The latter will represent the most defective metal areas. The average thickness of the passivating oxide coating formed upon the contact between the surface Al and the atmosphere is 2–4 nm [16]. At such a coating thickness, from 5 to 10 aluminum oxide layers are located over the metal surface. This means that the observed surface relief and structure of the passivating oxide coating must replicate in most cases

the relief and structure of a metallic aluminum particle located under its surface to a considerable extent. In this case, the passivating oxide coating located over the amorphous splices at the boundaries of crystalline grains will have the most defective structure. The destruction of the passivating oxide coating upon the contact between particles and water begins just from these areas.

This conclusion is confirmed by the SEM photos (Fig. 2a) of the surface of aluminum powder particles, which were oxidized by water and taken from the reactor after the initial oxidation stage was terminated. Reaction products escape (such as pimples and rollers), which proves the existence of through POC defects (pores and microcracks), are observed along the boundaries of areas with a size of 100–200 nm, which corresponds to the sizes of aluminum microcrystallites composing a particle according to X-ray diffraction data.

Hence, the oxidation reaction product, namely, aluminum hydroxide is accumulated in the areas of through defects formed in the oxide coating during the initial oxidation process. According to the work [20], the contact of aluminum hydroxide with metallic aluminum leads to the reaction between them with the formation of hydrogen and aluminum oxide (i.e., aluminum hydroxide rehydrolysis). The formed aluminum oxide is much less permeable for water than hydroxide. This seems to be a reason for the evolution of the initial oxidation stage into the induction stage: the defects opened upon contact with water are closed by the newly formed oxide, and the formation of new defects requires time (the time of the hydration and further local dissolution of the coating).

The initial oxidation stage can be most pronouncedly observed when the chemical activation with alkali and alkali-earth metal oxides and hydroxides is used (Fig. 1c). In this work, we shall demonstrate the mechanism of this effect using the activator CaO as an example. Medium high pH (12.5) stipulated by the dissolution of calcium hydroxide provides the dissolution of the formed aluminum oxidation product, i.e., aluminum hydroxide by the reaction



Dissolved aluminum hydroxide reacts with calcium hydroxide to form calcium hydroxoaluminates $3\text{CaO} \cdot \text{Al}_2\text{O}_3 \cdot 6\text{H}_2\text{O}$ ($2\text{Al}(\text{OH})_4^- + 3\text{Ca}^{2+} + 4\text{OH}^- \rightarrow 3\text{CaO} \cdot \text{Al}_2\text{O}_3 \cdot 6\text{H}_2\text{O}$), which are detected by X-ray diffraction at the initial stages of the oxidation process. The amount of aluminum oxidized at the initial oxidation stage correlates with the CaO activator amount introduced into the system (Table 1). Thus, for example, 0.13 g of calcium hydroxide are formed according to stoichiometry in the oxidation of aluminum powder (2 g) in water (8 mL) upon the introduction of CaO in the amount of 5% of the aluminum mass (0.1 g). This amount of calcium hydroxide corresponds to 0.09 g of

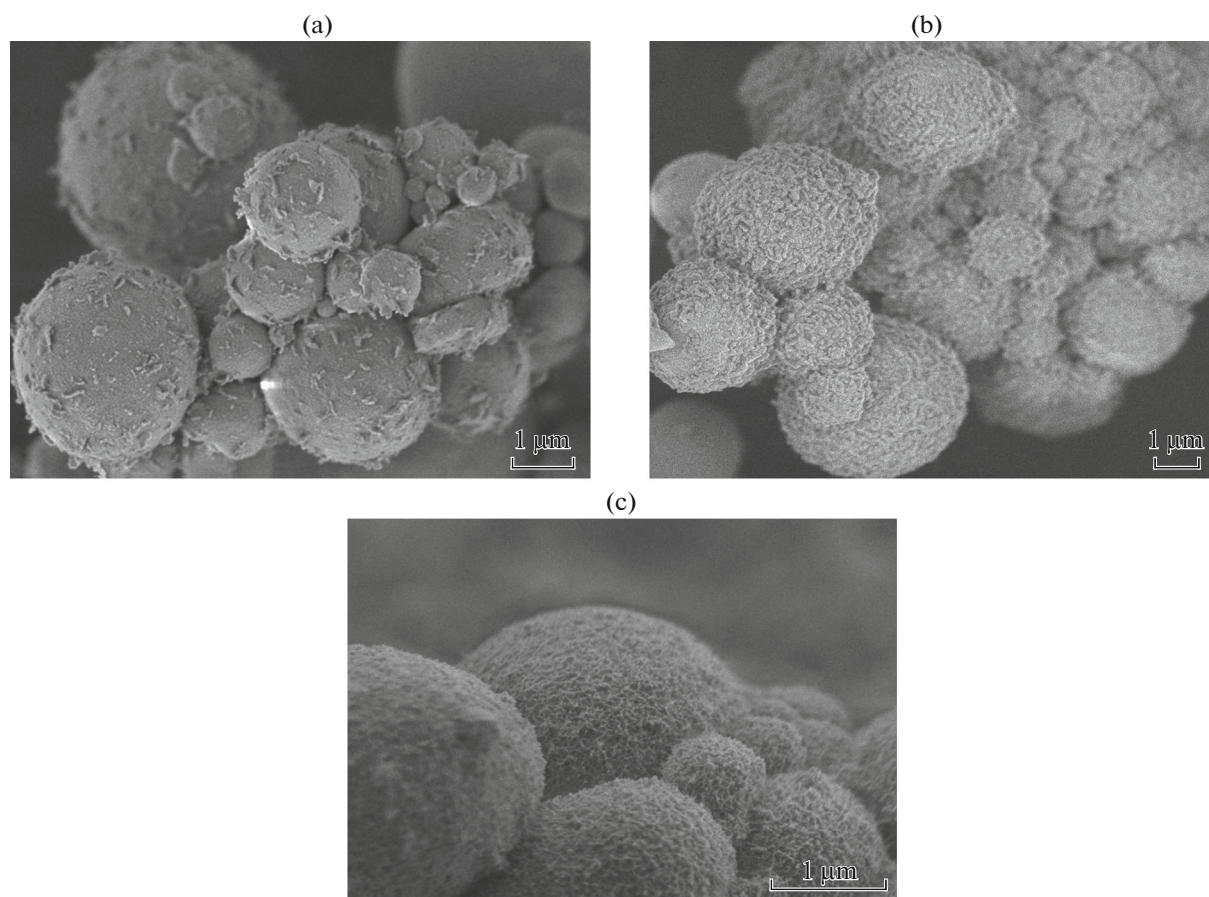


Fig. 2. SEM microphotos for the products sampled from the reactor at the moments specified in Fig. 1a for the reaction of aluminum oxidation by water at an oxidation degree of (a) 1.1, (b) 8, and (c) 17%, Al : H₂O of 1 : 4, and *T* of 40°C.

aluminum hydroxide (according to the reaction $3\text{Ca}(\text{OH})_2 + 2\text{Al}(\text{OH})_3 \rightarrow 3\text{CaO} \cdot \text{Al}_2\text{O}_3 \cdot 6\text{H}_2\text{O}$); 0.09 g of aluminum hydroxide is formed in the oxidation of 0.03 g of aluminum, which is 1.5% of the initial aluminum mass. According to experimental data, just this amount of aluminum is oxidized at the initial oxidation stage in the considered experiment. The SEM photos obtained for the oxidized aluminum powder sample taken immediately after the initial oxidation stage demonstrate the existence of lamellar crystals with linear sizes of several microns (Fig. 3). The comparison of the results of SEM and X-ray diffraction allows us to presume that the lamellar crystals visible in the SEM photos represent calcium hydroxoaluminates. It should be noted that the crystals are located outside the oxidized particles, and this does not allow them to screen the aluminum surface, so the initial oxidation in the presence of the activator is more intensive than without activation. When an appreciable portion of the introduced activator is converted into calcium hydroxoaluminates (in the solid and partially dissolved state), the aluminum gel formed covers oxide coating defects. In this case, the initial oxidation stage is terminated to evolve into the induction stage.

The induction stage is associated with the hydrolysis of the passivating oxide coating by almost all the researchers [1, 4, 17–20]. At this stage, Al–O–Al structural bridges are destructed with the formation of Al–OH bonds and, at the same time, pH of the reaction medium is observed to grow to stabilize within a range from 7 to 9.5 (depending on the process conditions). It has been noticed that this parameter at a constant amount of used distilled water is proportional to the amount of Al powder, which is mixed with water and forms dispersion [4], i.e., proportional to the particle surface area, which is in contact with water. In the paper [4], it has been demonstrated that ASD-grade aluminum powders containing the greatest amount of chemisorbed OH groups in the passivating oxide coating (determined by derivatography in combination with thermal desorption mass spectrometry) have the shortest induction period, and pH in the mixtures of such powders with water attains high values.

According to the work [20], OH groups formed on the external surface of a particle as a result of its interaction with water diffuse from the water–oxide coating interface towards the oxide coating–aluminum interface to form structural hydroxides in the coating

Table 1. Correlation between the introduced activator amount and the amount of aluminum oxidized at the initial oxidation stage

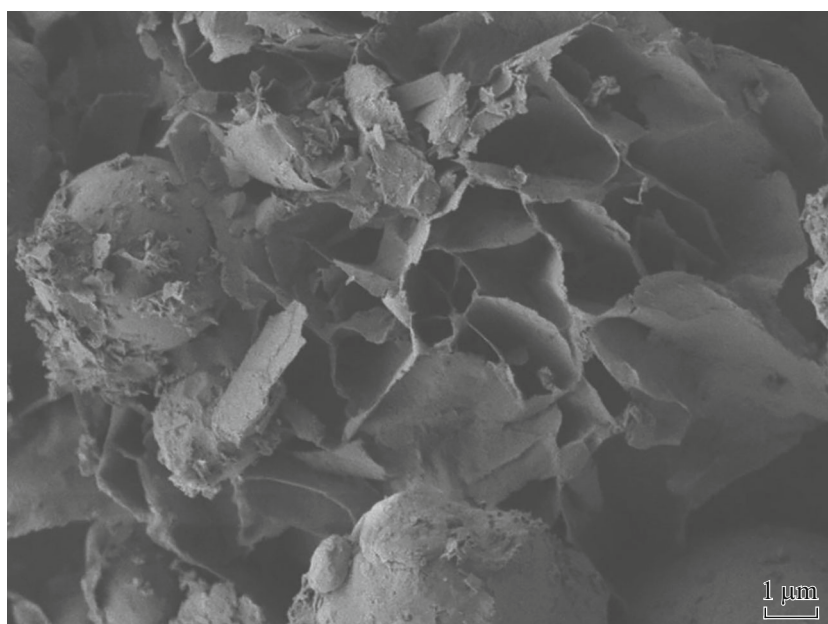
Introduced activator amount, % of total Al mass	Amount of Al bonded into $3\text{CaO} \cdot \text{Al}_2\text{O}_3 \cdot 6\text{H}_2\text{O}$ at the given activator amount, if the activator is completely spent on the formation of aluminates, % of total Al mass	Amount of aluminum oxidized at the initial oxidation stage, % of total Al mass (found via the integration of experimental hydrogen release rate curves)
5	1.5	1.5 ± 0.8
8	2.4	2.7
20	6	4.8

volume. In this work, it is presumed that the diffusion of OH groups is appreciably accelerated with an increase in the amount of defects in aluminum oxide. When OH groups attain metallic aluminum, aluminum hydroxide is subjected to rehydrolysis. The formed aluminum oxide will increase the POC thickness and can be hydrolyzed again. The process of growth in the oxide coating under the initial POC present on aluminum powders in the as-received state is extremely slow (at room temperature, the oxide coating thickness increases from 4.5 to 5 nm after 5 h of contact with water [20]). The intensification of this process is promoted by the destruction of the oxide coating. According to the work [15], the formed hydrogen accumulated under the oxide coating may lead to its destruction in case the hydrogen formation rate is higher than the rate of its diffusion. However, in our opinion, the accumulation of hydrogen bubbles is very unlikely, as the effective diffusion coefficient of OH groups in oxide is much lower (according to [20],

it attains $\sim 10^{-17} \text{ cm}^2/\text{s}$), though the oxide coating is an essential hindrance for the formed hydrogen (it follows from the analysis of the results [24, 25] that the coefficient of hydrogen diffusion in oxide is $10^{-13} - 10^{-14} \text{ cm}^2/\text{s}$). It seems that the termination of the induction period is associated with the hydrolyzed POC being locally dissolved in the most defective areas.

The use of the activator CaO provides the possibility to shorten the induction period, as the solubility of aluminum hydroxide and the rate of its dissolution by reaction (1) at higher pH values appreciably increase. The induction period evolves into the intensive oxidation stage, when the amount of through defects is accumulated, and the rate of their formation exceeds the rate of healing (as a result of rehydrolysis).

The use of ultrasonic activation also provides the possibility to shorten the induction period due to the mechanical effect produced on the passivating oxide coating by the microflows appearing upon the collapse

**Fig. 3.** SEM microphotos for the products obtained after the initial oxidation in the presence of CaO in the amount of 5% of the Al mass.

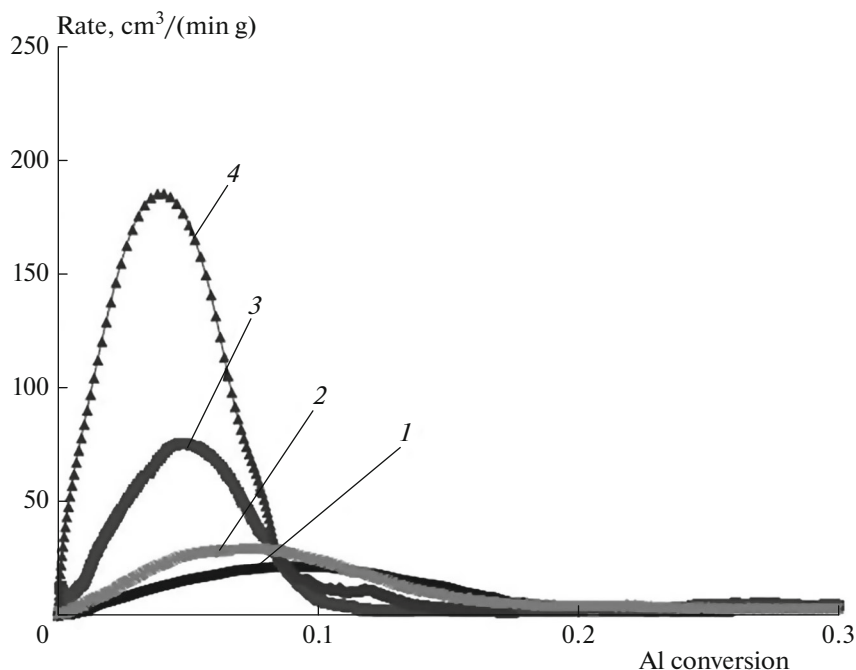


Fig. 4. Hydrogen formation rate versus metallic aluminum conversion at Al : H₂O of 1 : 4. Oxidation process was performed in the isothermic regime at a temperature of (1) 55°C, (2) 60°C, (3) 70°C, and (4) 100°C.

of cavitation bubbles formed under the influence of ultrasound and the heating of the mixture by an ultrasonic field [9].

Intensive Oxidation and Oxidation Damping Stages

In the absence of activation, the time dependence of the gas release rate has one maximum (Fig. 1a). The analysis of microphotos for the particles taken from the reactor at the beginning of the intensive oxidation stage shows that some rollers observed on the surface (Fig. 2a) are united into a dense network of rollers representing the escapes of aluminum oxidation products onto the surface (Fig. 2b). This indicates that point through defects turn into cracks growing in length during the oxidation process, and their amount per unit surface area increases. The rollers (aluminum hydroxide) that are formed cover a greater part of the surface of aluminum particles (Fig. 2b). The X-ray diffraction analysis of oxidation products shows that only amorphous aluminum hydroxide is formed at this process stage without activation. It seems that aluminum hydroxide micellae, which do not hamper the transport of water to the oxidized metal, fill the volume of a defect, and are exposed on the surface of a particle with time to form rollers, are formed in the process of oxidation in the areas of through defects. The growth of rollers then leads to the formation of a water-saturated gel covering the surface of a particle.

The gel loses excess water molecules with time to become structured, i.e., sustains aging (Fig. 2c), and

loses the ability to transmit water to the oxidized metal surface. Let us note that the rate of aluminum oxidation by water grows with an increase in the reaction medium temperature (the accumulation of aluminum gel), but this simultaneously accelerates gel structuring, which respectively reduces the access of water to the non-oxidized metal and the metal oxidation rate and leads to the stoppage of the oxidation process. As a result, the formed hydrogen release maximum shifts towards lower metal oxidation degrees with an increase in the oxidation process temperature (Fig. 4). A similar decrease in the aluminum oxidation rate with time was observed in the work [17] in the study of mechanochemically activated aluminum powders; the authors explained this by the hydroxide layer having sustained compaction, as evidenced by the SEM photos of a hydroxide shell cross section.

The mechanism of the aluminum oxidation at its different stages for nanosized particles was studied in the work [18]. According to this work, aluminum oxidation products are formed in the defective POC areas and are amorphous, thus corresponding to the conclusions made in this work. However, a boehmite shell is formed around the aluminum core during the oxidation process in the case of nanosized aluminum particles [18], and this shell is hollow, as the complete oxidation of aluminum can be attained for such particles. Hence, the products of the oxidation of nanosized aluminum particles represent hollow nanospheres [18]. In the case of micron aluminum particles studied in this work, the ultimate metal oxidation degree detect-

able for a reasonable time of observation (up to several days) in the absence of activation does not exceed 30%, and the reaction product is particles with a metallic core and a shell of amorphous aluminum hydroxide formed after the aluminum hydroxide gel is dried.

The mechanism proposed above in the present work for the formation of the hydroxide layer covering an aluminum particle is implemented in all the thermal regimes in the absence of activation. The kinetic dependence of gas release under these conditions has one maximum. When ultrasonic or chemical activation (small CaO additives) is used in the quasi-isothermic oxidation regime, the kinetic curve of the hydrogen formation rate has several maxima (as a rule, two). To explain the nature of the second maximum, we performed a stagewise SEM and X-ray diffraction study of oxidation products using the method described in Section 2.

The SEM photos of oxidation products obtained in the quasi-isothermic regime with chemical activation (Fig. 5, the moments of sampling for electron microscopy are denoted with letters in Fig. 1b) show that the oxidation process in the first maximum follows the mechanism similar to the mechanism observed in the case of oxidation without activation: at the beginning of the intensive oxidation stage, the products are precipitated in the areas of through defects (Fig. 5a), thereupon the formed aluminum hydroxide completely covers the surface of oxidized particles, thus hampering the access of water to the non-oxidized metal (Fig. 5b). Starting at a certain moment (denoted by the letter *c* in Fig. 1b), lamellar aluminum hydroxide structures representing the precursors of aluminum hydroxide crystals can be observed in the electron microscopic photos. Figure 5d shows that the growth of aluminum hydroxide crystals occurs in the radial direction from the surface of an oxidized particle coated with an aluminum hydroxide gel layer. It is obvious that aluminum hydroxide is transported from the oxidized aluminum surface to the growing crystals at distances corresponding to the sizes of the crystallites (of nearly 10 μm). The transport of aluminum

hydroxide is generally performed by $\text{Al}(\text{OH})_4^-$ ions, as the dissolved aluminum hydroxide at $\text{pH} > 7$ is mainly presented by these ions [23]. The mass transfer of Al hydroxide will hamper the accumulation of oxidation products on the surface of aluminum particles and, correspondingly, promote an increase in the oxidation rate. It should be noted that aluminum hydroxide crystals are always observed in the SEM photos, if the second maximum is present in the gas release curve in experiments. This allows us to hypothesize that the repeated growth of the hydrogen release rate (the second maximum) is associated with the transition of aluminum hydroxide from a gel state (covering the surface of metallic aluminum) into a crystalline state (at a distance from the surface).

A necessary precondition for the formation of crystallization nuclei and their further growth to the crystalline forms of aluminum hydroxide is the appearance of dissolved Al hydroxide oversaturation areas. It seems that the oversaturation of the solution at a distance from the oxidized particles is provided by the temperature factor. Due to the intensive release of heat during the oxidation of aluminum by water, the local temperature of the liquid near the oxidized aluminum surface proves to be higher than at a distance from this surface. When the medium has $\text{pH} > 7$ (general conditions), the solubility of aluminum hydroxide grows with an increase in the temperature of reagents [26, 27].¹ The solution near the oxidized surface has maximum concentration and temperature. The transportation of reaction mixture microvolumes by liberated hydrogen and/or due to convection appearing in the temperature field leads to the warm saturated solution from the near-surface zone occurring in the peripheral areas with a lower temperature. This results in its cooling to a given local temperature and the transition into the oversaturated form. Hence, the oversaturated solution areas with the nucleation and further growth of aluminum hydroxide crystals appear at a distance from the oxidized aluminum surface. Let us note that the dissolved aluminum hydroxide concentration gradient appearing due to the temperature gradient grows with an increase in pH of the medium.² An increase in the concentration gradient between the oxidized aluminum surface and the areas far from this surface provides a more vigorous nucleation and growth of crystals at the intensive oxidation stage.

As shown by SEM data, aluminum hydroxide crystals surrounding a particle are near in size (the average length of particles reaches several microns) at the terminal stage of the oxidation process (Fig. 5d). This indicates that the nucleation of crystals occurs within a certain limited time period, after which further nucleation is ceased, and the growth of already formed crystals is observed alone. The formation of crystal nuclei seems to occur at the intensive oxidation stage, when the near-surface rate and temperature reach rather high values, due to which the gradient of temperature and dissolved hydroxide concentration is established. At this stage, the formed nuclei of aluminum hydroxide crystals still have a small surface area and do not provide any appreciable flow of aluminum hydroxide from the surface of aluminum particles to

¹ The estimates of the aluminum hydroxide solubility by the data [26] show that the solubility is 40 times greater when the temperature increases from the room temperature to 100°C at neutral pH.

² The solubility estimates by the data [26] show that the change in pH from 7 to 12.5 leads to an appreciable increase in the $\text{Al}(\text{OH})_4^-$ concentration gradient even at a small temperature gradient (30°C) in the reaction mixture between the near-surface layer of an oxidized particle (55°C) and the nucleation zone (25°C): it attains 2×10^{-7} mol/L at neutral pH and 4×10^{-2} mol/L at pH of 12.5.

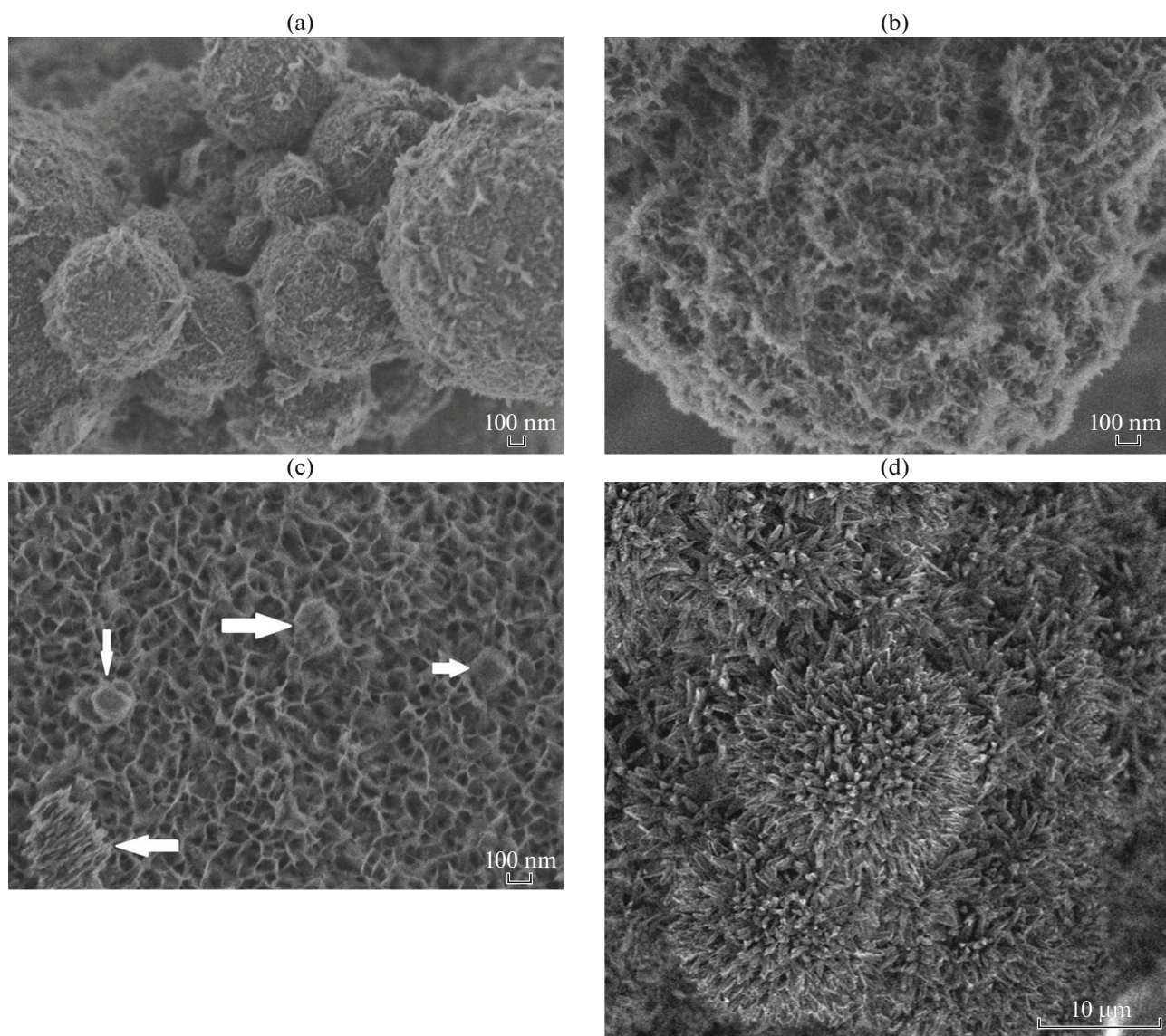


Fig. 5. SEM microphotos for the products of the reaction of aluminum oxidation by water in the presence of CaO at Al : H₂O of 1 : 11 and *T* of 70°C. Samples were taken from the reactor at a conversion of (a) 0.8% (amorphous Al(OH)₃), (b) 15% (amorphous Al(OH)₃), (c) 23% (the beginning of the formation of crystalline Al(OH)₃, crystal precursors are marked with arrows), and (d) 85% (crystalline Al(OH)₃). Moments of sampling for electron microscopy are denoted in Fig. 1b by letters.

the crystallization nuclei. Correspondingly, gel-like oxidation products inhibit the reaction, being accumulated on the oxidized aluminum surface, and the oxidation rate is reduced, thus leading to a decrease in the local temperature near the oxidized surface and the dissolved hydroxide concentration gradient. This leads to an oversaturation in the solution at a distance from the particles is reduced, and no new aluminum hydroxide nuclei are formed. The intensive oxidation stage evolves into a process damping stage. However, the growth of already formed crystal nuclei occurs at this stage, and their surface area is enlarged, thus increasing the mass transfer of aluminum hydroxide from the surface of aluminum particles to crystalliza-

tion nuclei. As a result, the reactivation of the aluminum oxidation process, i.e., a repeated increase in the gas release rate, may occur. Let us note that no nucleation takes place after reactivation (i.e., during the passage through the second maximum), as oversaturation in the solution is reduced due to the growth of already formed crystals.

The growth of aluminum hydroxide crystals at the process damping stage may be rather intensive only with activation. In fact, the oriented flow of dissolved aluminum hydroxide towards the surface of crystals is formed, as the dissolved aluminum hydroxide concentration near the surface of growing crystals is lower (tends to zero) than at a distance from them. The value

of this flow is determined by the difference between the dissolved aluminum hydroxide concentrations near the aluminum surface (where the concentration is close to the saturated solution concentration) and near the surface of growing Al hydroxide crystals. Since the solubility of the latter appreciably grows with increasing pH [26, 27], the dissolved aluminum hydroxide flow towards the growing crystals also increases, even at the process damping stage, when the temperatures near aluminum surface and in the mixture volume become close to each other. The mass transfer of dissolved aluminum hydroxide to the growing crystals occurs due to diffusion, thermal diffusion, and the above-mentioned convection and hydrogen bubbles.

The mechanism of the aluminum oxidation process activated with calcium hydroxide was also studied in the work [19]. A distinction of our work from the paper [19] is a relatively small amount of used calcium hydroxide in the present work (less than 6.5% of the Al mass (5% for CaO)) in comparison with the amount used in the work [19] (more than 20%). The first maximum in the kinetic gas release curve from the work [19] seems to correspond to the initial oxidation, which was observed by us and described in the previous section. The authors explain this maximum by the formation of calcium aluminate. In this work, it is presumed that hydrogen is liberated during the passage through the first maximum due to the formation of calcium hydroxoaluminates by the reaction $3\text{Ca}^{3+} + 2\text{Al}(\text{OH})_4^- + 8\text{H}_2\text{O} \leftrightarrow \text{Ca}_3\text{Al}_2(\text{OH})_{12} + 6\text{H}_2$. However, according to the contemporary notions [28, 29], the formation of hydroxoaluminates is not accompanied by the formation of hydrogen. The second maximum in the work [19] is associated with the growth of aluminum hydroxide crystals, and this does not contradict the mechanism proposed by us for the oxidation of aluminum at a small activator amount.

It should be noted that the kinetic gas release curve for the oxidation of aluminum with ultrasonic activation in the isothermic regime within a temperature range of 20–70°C also has two maxima (Fig. 6). The SEM study of the oxidation process at its different stages shows that aluminum hydroxide crystals can be observed in the SEM photos during the passage through the second gas release maximum as in the case of chemical activation. It seems that ultrasound promotes the formation of Al hydroxide crystal nuclei and their further growth due to the intensification of mass transfer. The ability of an ultrasonic field to accelerate the formation of nuclei [30] and the growth of crystals [31] even at small solution oversaturation degrees is widely known. The process of crystallization in an ultrasonic field (sonocrystallization) is intensively studied [30, 31]. The ultrasonic activation of nucleation and crystal growth is stipulated by the collapse of cavitation bubbles appearing during the propagation of an ultrasonic wave through the solution [32].

The time dependence of the H₂ liberation rate has one maximum, and the metal is almost completely oxidized for several minutes, when the oxidation of aluminum is performed with chemical activation (addition of CaO) in the heat accumulation regime (i.e., in combination with thermal activation) or with the simultaneous use of ultrasonic and chemical activation in the quasi-isothermic regime (Fig. 1c). SEM studies show that the products of oxidation in these cases are nanosized aluminum hydroxide crystals (Fig. 7). The observed formation of a great number of small crystals indicates that nucleation is more intensive here than in the oxidation process with chemical or ultrasonic activation alone. It seems that the application of chemical activation in combination with thermal or ultrasonic activation provides the possibility to attain higher degrees of oversaturation in the solutions, where aluminum hydroxide crystallizes. In fact, the simultaneous use of two activation methods provides the fastest and most intensive destruction of the passivating oxide coating, and this in turn leads to an increase in the gas liberation rate with an associated increase in the heat liberation rate. Hence, the temperature gradient created at the intensive oxidation stage between the surface of a particles and the ambient medium is higher than for the separate application of activation methods. As shown above, a high temperature gradient in combination with high pH of the medium provides a greater solution oversaturation degree at a distance from an oxidized particle and, consequently, a greater number of crystallization nuclei are formed. The simultaneous formation of a great amount of nuclei and an increased possibility for the transportation of dissolved hydroxide (at the expense of the used activation methods) lead to the formation and growth of a great amount of nanosized hydroxide crystals. It seems that the mass transfer of aluminum hydroxide from the surface of particles to crystallization nuclei with the resulting transformation of amorphous hydroxide into the crystalline phase begins to play an essential part in this case much before the amorphous aluminum hydroxide shell attains the thickness, at which it becomes an appreciable hindrance for the access of water to the surface of metallic aluminum. As a result, the two maxima in the kinetic gas liberation curve merge into a single maximum, where one of them may be observed in the form of a more or less pronounced shoulder.

The proposed oxidation process mechanism allows us to understand why the short-term effect of ultrasound is sufficient to activate the process with an ultrasonic field in the presence of the activator CaO at the beginning of the intensive oxidation stage [9]. In this case, an ultrasonic field promotes the formation of aluminum hydroxide crystal nuclei, and the further high mass transfer rate is provided by an increase in the solubility of aluminum hydroxide in the presence of CaO.

Hence, it follows from the information stated in this section that the fast and complete oxidation of metal is implemented when meeting the following.

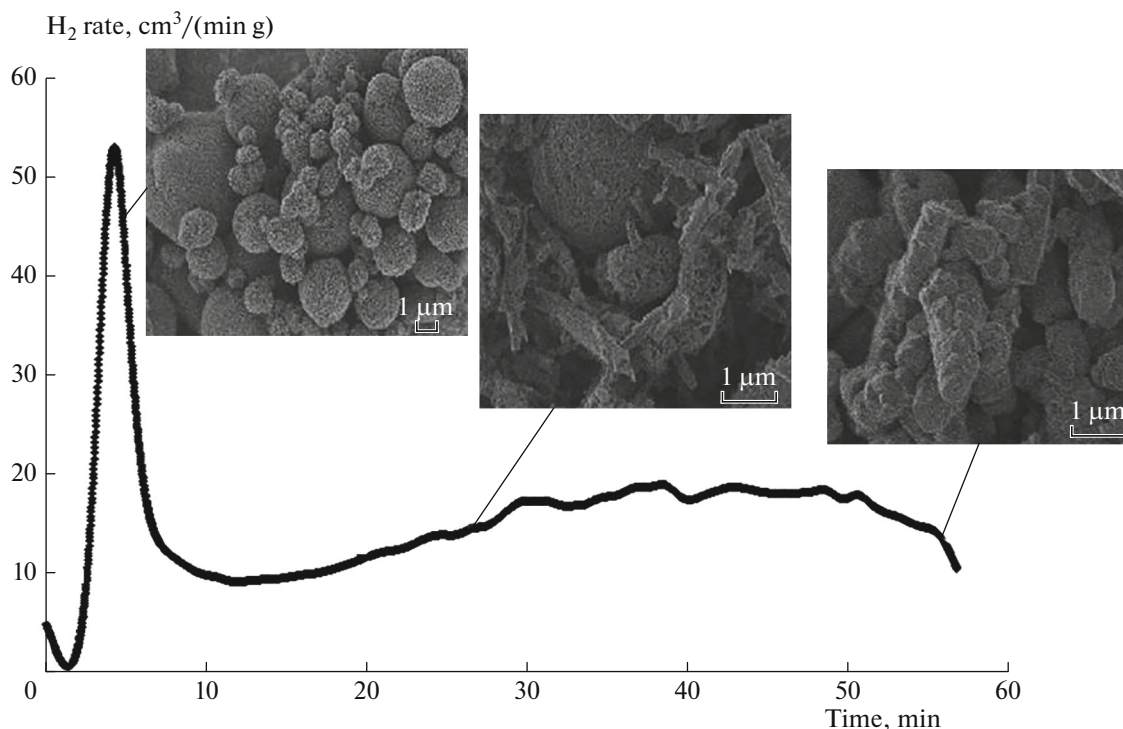


Fig. 6. Kinetic curve of the hydrogen liberation rate with the products of aluminum powder oxidation by water. Process was performed using the activation with an ultrasonic field at a temperature of 70°C.

(1) The conditions for the fast destruction of the passivating oxide coating are created. This is promoted by both chemical (CaO) and ultrasonic activation [1, 8–12]. The induction period is shortened in this case.

(2) At the intensive oxidation stage, the process rate is sufficiently high to provide a necessary gradient of temperatures between the surface of an oxidized particle and the medium at a distance from this particle and, correspondingly, the creation of an oversaturated concentration for the dissolved aluminum hydroxide forms in the areas distant from the surface of the oxidized metal.

(3) The rate of the mass transfer of dissolved aluminum hydroxide from the oxidized surface of aluminum particles to crystallization nuclei is higher than the rate of decrease in the permeability of the hydroxide shell around the oxidized particles for water. The permeability for water is decreased due to an increase in the shell thickness and the structuring newly formed hydroxide (i.e., adding in the order *micellae* > *water-saturated gel* > *structured hydrogel*).

It follows from the data considered in the present paper that the structure of formed oxidation products can be predicted from the obtained time dependences of the hydrogen liberation rate (their shape and the aluminum conversion found from them) with a high degree of precision independently of the method used for the activation (e.g., ultrasonic or chemical) of the oxidation process of aluminum powders with micro-

sized particles (in this case, all the gas liberation curves can be classified into three groups):

—The first group of kinetic hydrogen release curves is characterized by the only gas liberation maximum; in this case, the process is almost ceased after the passage through the maximum and the oxidation of a relatively small (up to 30%) Al amount and further occurs at an extremely low temporally decreasing rate of several $\text{cm}^3/(\text{min g})$ and smaller (Fig. 1a). The maximum rate attainable in the oxidation process may be both extremely low of several tens of $\text{cm}^3/(\text{min g})$ and rather high of nearly $500 \text{ cm}^3/(\text{min g})$ and even more. Particles with a metallic core with a metal structure corresponding to the structure of an initial particle and a shell composed of amorphous $\text{Al}(\text{OH})_3$ with a thickness of up to several hundreds of nanometers are formed in such a process. The specific surface area of oxidation products exceeds $60 \text{ m}^2/\text{g}$ for the oxidized sample (metal + Al hydroxide) and $110 \text{ m}^2/\text{g}$ per formed hydroxide alone.

—The second group is characterized by a high conversion of metallic aluminum and the presence of two (and three in some cases) maxima in the kinetic hydrogen liberation curve (Fig. 1b). The aluminum oxidation rate usually attains several tens of $\text{cm}^3/(\text{min g})$. In this case, the oxidation products are aluminum hydroxide crystals with a size of several microns (Fig. 5d) and a specific surface area of nearly $15 \text{ m}^2/\text{g}$.

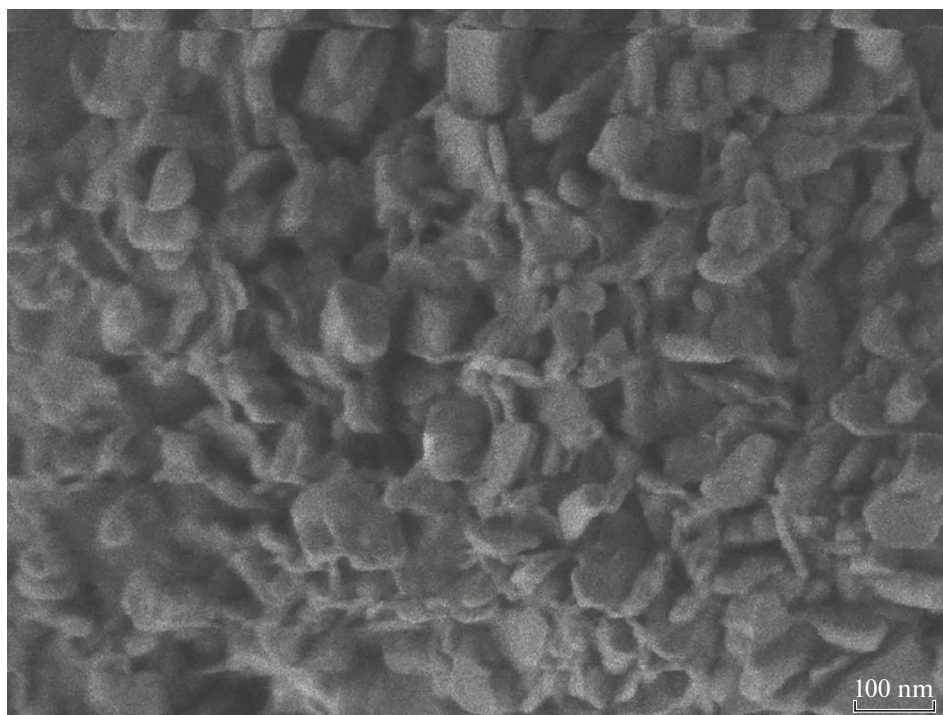


Fig. 7. SEM microphotos for the products of the reaction of aluminum oxidation by water with the simultaneous application of ultrasonic and chemical (CaO) activation.

—The third group is characterized by the fast oxidation process and the complete oxidation of metallic aluminum (the oxidation rate grows by 1–3 orders of magnitude in comparison with the second group). The kinetic curves have the only gas liberation maximum (Fig. 1c). Nanosized aluminum hydroxide crystals with a particle size of 20–150 nm and a specific surface area of more than 40 m²/g are formed in this case (Fig. 7).

Change in pH of the Medium during the Aluminum Oxidation Process

The medium pH measurements performed in this work have provided the possibility to confirm and refine the above described mechanism of the aluminum oxidation process. Here, it should be taken into account that the character of the pH–time dependences measured during the aluminum oxidation process is rather qualitative than quantitative, as no steady-state pH has been attained for the period of measurement.

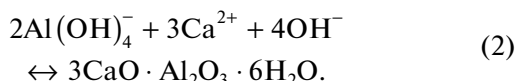
pH of the medium may both grow (Fig. 1a) and decrease (Figs. 1b and 1c) depending on its starting value upon the contact between the aluminum powder and water. It is known [33] that hydroxyl ions, which have different structures and are bonded to the surface in different fashions, are formed in the process of the hydration on the surface of the aluminum oxide contacting water. The surface charge settling mechanism is based on the phenomenon of the adsorption and

desorption of protons by active sites [33]. The surface of aluminum hydroxide is amphoteric and may act as both a Brønsted acid and base depending on pH of the medium. The surface is positively charged when pH is lower than the value corresponding to the zero charge point (ZCP), and negatively charged at higher pH. The ZCP value may variate from ~7 to ~10 depending on the type of aluminum oxide [33].

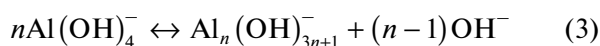
The kinetic characteristics of the surface charge settling process can be observed when studying the medium pH settling kinetics in an aluminum powder–water mixture. The kinetic curve of change in pH of the medium in the aluminum oxidation process at neutral starting pH is illustrated in Fig. 1a (curve 2). As mentioned above, the surface is positively charged in this case, and this is accompanied by an increase in pH of the medium. Curve 2 for pH in Fig. 1a has a deflection at the time moment of ~10 min corresponding to the most intensive gas liberation. This deflection is likely to be associated with the dissolution of newly formed aluminum hydroxide by reaction (1). The kinetic aluminum oxidation curves and the change in pH of the medium at starting pH 12.5 are shown in Figs. 1b and 1c. Under these conditions, the oxide coating surface is negatively charged, and pH of the medium decreases at the initial time moment.

In addition to the above described process of change in pH of the medium due to the surface charging of the oxide coating of aluminum, a decrease in pH at the initial oxidation stage at an alkaline start-

ing pH is caused by the dissolution of formed hydroxide by reaction (1) and the formation of calcium aluminates:



When starting pH 12.5, the time dependence of pH of the medium at the intensive oxidation and reaction damping stages represents an invertible time dependence of the oxidation rate (Figs. 1b and 1c). A decrease in pH of the medium at the intensive oxidation stage is attended with the dissolution of aluminum hydroxide by reaction (1), and its increase, on the contrary, is associated with the linking of aluminum hydroxide into chains [23], being accompanied by the loss of OH^- ions by the reaction



and further crystallization, and, probably, is also associated with the partial dissolution of aluminates formed at the initial oxidation stage. Processes (1)–(3) occur simultaneously throughout the entire aluminum oxidation period. The resulting effect of these processes leads to steady-state pH determined by thermodynamic equilibrium in the $\text{Al}(\text{OH})_3\text{--H}_2\text{O--CaO}$ –calcium aluminates system with time. The deviation of pH from its steady-state value is maximal at the highest reaction rate moments, when the greatest amount of active newly formed aluminum hydroxide is synthesized. It seems that the rate of the dissolution of aluminum hydroxide by reaction (1) exceeds the rate of its structuring by reaction (3) and, correspondingly, pH of the medium deviates from its steady-state value towards smaller pH (Figs. 1b, 1c). After the oxidation process is terminated, pH of the medium attains a steady-state value with time. Let us note that an increase in pH of the medium at the induction stage in the presence of calcium aluminates (Fig. 1c) also seems to be associated with the trend of pH to a steady-state value for the $\text{Al}(\text{OH})_3\text{--H}_2\text{O--CaO}$ –calcium aluminates system [28].

Hence, pH of the medium deviates from its steady-state value for the given system during the intensive oxidation and tends to this value after the termination of intensive oxidation, when the activator CaO is used. Because the activation effect of CaO at the induction and intensive oxidation stages is determined by an increase in the solubility of aluminum hydroxide in the presence of this activator, the CaO amount sufficient to activate the process is 5% of the Al mass in most cases, and its increase to >5% does not lead to the change in the oxidation kinetics (except the initial oxidation stage, as shown above). However, as shown by our studies, the use of this activator in the amount of less than 5% leads to a decrease in the oxidation rate at the intensive oxidation stage. This seems to be associated with the fact that calcium aluminates formed at the initial oxidation stage can be partially dissolved by

reaction (2), thus increasing pH. Hence, the calcium aluminates formed serve as a buffer for OH^- ions, thus providing activation.

4. CONCLUSIONS

The application of the complex approach to studying the process of disperse aluminum oxidation by water with the use of electron microscopy and X-ray diffraction analysis and the kinetics of aluminum oxidation and change in pH of the medium in the process of oxidation has provided the possibility to detail the oxidation process mechanism in different regimes (including chemical (CaO addition) and ultrasonic activation). That the following has been demonstrated:

(1) The initial oxidation stage is stipulated by the existence of POC defects, which are impermeable for atmospheric oxygen and open upon contact with water. The areas of such defects are located under amorphous aluminum binding Al microcrystallites into a single particle.

(2) The induction stage is caused by the hydrolysis of the oxide coating.

(3) Aluminum hydroxide is formed at the intensive oxidation stage in the form of a water-saturated gel. When activation is used, the intensive oxidation stage is simultaneously the stage of the nucleation of aluminum hydroxide crystals.

(4) The oxidation damping stage is associated with the competition between the two processes, such as (i) the growth of the gel layer in thickness with a simultaneous decrease in its permeability for water and (ii) the growth of aluminum hydroxide crystals with the intensification of the mass transfer of aluminum hydroxide from the oxidized surface to the area of crystallization during the growth of crystals. In the case when the second process proves to be more intensive than the first process, the damping stage newly evolves into the intensive oxidation stage. The stages may alternate with each other up to the complete oxidation of aluminum.

The revealed interrelation between the structure of formed oxidation products and the process kinetics, in all appearances, takes place not only when the mentioned activation methods are used, but also can be extended to the other activation methods and conditions of disperse aluminum oxidation by water.

REFERENCES

1. M. N. Larichev (L. M. Nikolaevich), in *Metal Nanopowders: Production, Characterization, and Energetic Applications*, Ed. by A. Gromov and U. Teipel (Wiley-VCH, Weinheim, 2014), p. 163. <https://doi.org/10.1002/9783527680696.ch8>
2. H. Z. Wang, D. Y. C. Leung, M. K. H. Leung, et al., *Renewable Sustainable Energy Rev.* 13, 845 (2009). <https://doi.org/10.1016/j.rser.2008.02.009>

3. E. I. Shkolnikov, A. Z. Zhuk, and M. S. Vlaskin, *Renewable Sustainable Energy Rev.* 15, 4611 (2009).
<https://doi.org/10.1016/j.rser.2011.07.091>
4. M. N. Larichev, O. O. Laricheva, I. O. Leipunskii, et al., *Izv. Akad. Nauk, Energ.*, No. 5, 125 (2007).
5. J. M. Bergthorson, Y. Yavor, J. Palecka, et al., *Appl. Energy* 186, 13 (2017).
<https://doi.org/10.1016/j.apenergy.2016.10.033>
6. A. Z. Zhuk, M. S. Vlaskin, A. V. Grigorenko, et al., *J. Ceram. Proc. Res.* 17, 910 (2016).
7. S. A. Kislenco, M. S. Vlaskin, and A. Z. Zhuk, *Solid State Ionics* 293, 1 (2016).
8. M. N. Larichev, N. S. Shaitura, and O. O. Laricheva, *Russ. J. Phys. Chem. B* 2, 757 (2008).
<https://doi.org/10.1134/S1990793108050175>
9. M. N. Larichev, N. S. Shaitura, V. N. Kolokol'nikov, et al., *Izv. Akad. Nauk, Energet.*, No. 2, 85 (2010).
10. N. S. Shaytura, M. N. Larichev, O. O. Laricheva, et al., *Curr. Appl. Phys.* 10 (Suppl. 2), S66 (2010).
<https://doi.org/10.1016/j.cap.2009.11.044>
11. M. N. Larichev, N. S. Shaitura, V. N. Kolokol'nikov, et al., *Perspekt. Mater.*, No. 9, 289 (2010).
12. M. N. Larichev, O. O. Laricheva, N. S. Shaitura, et al., *Izv. Akad. Nauk, Energ.*, No. 3, 66 (2012).
13. A. A. Gromov, A. P. Il'in, U. Foerter-Barth, et al., *Combust., Explos., Shock Waves* 42, 177 (2006).
14. M. N. Larichev, O. O. Laricheva, I. O. Leipunskii, et al., *Khim. Fiz.* 25 (10), 72 (2006).
15. Z. Y. Deng, J. M. F. Ferreira, Y. Tanaka, and J. Ye, *J. Am. Ceram. Soc.* 90, 1521 (2007).
<https://doi.org/10.1111/j.1551-2916.2007.01546.x>
16. A. Fernandez, J. C. Sanchez-Lopez, A. Caballero, et al., *J. Microsc.* 191, 212 (1998).
<https://doi.org/10.1046/j.1365-2818.1998.00355.x>
17. S. S. Razavi-Tousi and J. A. Szpunar, *Electrochim. Acta* 127, 95 (2014).
<https://doi.org/10.1016/j.electacta.2014.02.024>
18. A. S. Lozhkomoiev, E. A. Glazkova, O. V. Bakina, et al., *Nanotechnology* 27, 205603 (2016).
<https://doi.org/10.1088/0957-4484/2720/205603>
19. S. Kanehira, S. Kanamori, K. Nagashima, et al., *J. Asian Ceram. Soc.* 1, 296 (2013).
<https://doi.org/10.1016/j.jascer.2013.08.001>
20. B. C. Bunker, G. C. Nelson, K. R. Zavadil, et al., *J. Phys. Chem. B* 18, 4705 (2002).
<https://doi.org/10.1021/jp013246e>
21. E. I. Shkolnikov, N. S. Shaitura, and M. S. Vlaskin, *J. Supercrit. Fluids* 73, 10 (2013).
<https://doi.org/10.1016/j.supflu.2012.10.011>
22. P. A. Rebinder and E. D. Shchukin, *Sov. Phys. Usp.* 15, 533 (1972).
<https://doi.org/10.3367/UFNr.0108.197209a.0003>
23. J. Zang, M. Klasky, and B. C. Letellier, *J. Nucl. Mater.* 384, 175 (2009).
<https://doi.org/10.1016/j.jnucmat.2008.11.009>
24. W. H. Song, J. J. Du, Y. L. Xu, et al., *J. Nucl. Mater.* 246, 139 (1997).
[https://doi.org/10.1016/S0022-3115\(97\)00146-3](https://doi.org/10.1016/S0022-3115(97)00146-3)
25. I. B. Ulanovskiy, *Hydrogen Diffusion and Porosity Formation in Aluminium* (MISIS, Moscow, 2015) [in Russian].
26. I. L. Khodakovskii, L. V. Katorcha, and N. S. Kuyunko, *Geokhimiya*, No. 11, 1606 (1980).
27. X. Feng, Z. Baojie, and L. Chery, *J. Environ. Sci.*, No. 20, 907 (2008).
[https://doi.org/10.1016/S1001-0742\(08\)62185-3](https://doi.org/10.1016/S1001-0742(08)62185-3)
28. P. F. Romyantsev, V. S. Khotimchenko, and V. Sh. Nikushchenko, *Calcium Aluminates Hydration* (Nauka, Leningrad, 1974) [in Russian].
29. R. A. Lidin, et al., *Chemical Properties of Inorganic Substances*, 3rd ed. (Khimiya, Moscow, 2000) [in Russian].
30. M. D. Luque de Castro and F. Priego-Capete, *Ultrason. Sonochem.* 14, 717 (2007).
31. V. S. Nalajala and V. S. Moholkar, *Ultrason. Sonochem.* 18, 345 (2011).
32. M. A. Margulis, *Ultrasonics* 23, 157 (1985).
[https://doi.org/10.1016/0041-624X\(85\)90024-1](https://doi.org/10.1016/0041-624X(85)90024-1)
33. B. Kaspzyk-Hordern, *Adv. Colloid Interface Sci.* 110, 19 (2004).
<https://doi.org/10.1016/j.cis.2004.02002>

Translated by E. Glushachenkova